Analyst

PAPER

View Article Online
View Journal | View Issue

Cite this: *Analyst*, 2025, **150**, 2901

A validated experimental NMR parameter dataset of organic molecules to assist benchmarking of 3D structure determination methods†

Claire L. Dickson, *[a,b] Sadia Mohammed,[c] Lyrelle S. L. Jones,[c] Duncan J. Crick,[c] Wojciech Augustyniak,[c] Michael Beaumont,[c] Jan-Christoph Westerman,[c] Sarah Henshaw,[c] Steven T. Johnston,[c] Charles D. Blundell,[c] Martin Watson, [c] Zoltan Takacs[c] and Craig P. Butts *[a]

Received 3rd March 2025,
Accepted 16th May 2025

DOI: 10.1039/d5an00240k

rsc.li/analyst

Over 1000 accurately defined and validated experimental long-range proton–carbon ($^nJ_{CH}$) and proton–proton ($^nJ_{HH}$) scalar coupling constants, with assigned $^1H/^{13}C$ chemical shifts and their corresponding 3D structures are reported for fourteen relatively complex organic molecules. The experimental dataset comprises 775 $^nJ_{CH}$, 300 $^nJ_{HH}$, 332 ^1H chemical shifts and 336 ^{13}C chemical shifts, all validated against DFT-calculated values to identify misassignments. A subset of 565 $^nJ_{CH}$, 205 $^nJ_{HH}$, 172 ^1H chemical shifts and 202 ^{13}C chemical shifts from rigid portions of these molecules have been identified which could be particularly valuable for benchmarking computational methods for predicting NMR parameters. An exemplar application of this dataset is presented through benchmarking of the DFT mPW1PW91/6-311 g(dp) level of theory for computation of chemical shifts and scalar coupling constants and for testing scaling approaches for generating experimentally-relevant chemical shifts from DFT-computed magnetic shielding tensors.

Introduction

Collections of experimentally determined NMR parameters, primarily chemical shifts[1–3] but also scalar coupling constants,[1,4,5] have been an important feature in the development of methods for the determination of both 2D connectivity and 3D structure of molecules by NMR. The value of experimental datasets to the analytical community is widespread: acting as sources of data for developing and testing empirical methods, such as variations of the well-known Karplus equation,[6] and more recently machine-learning approaches[2,7–11] for predicting these NMR parameters. In recent years, they have been especially valuable in assessing the accuracy of quantum mechanical calculations of chemical shifts[12,13] and scalar coupling constants.[14,15] Methods for automated chemical structure validation and computer assisted structure elucidation (CASE)[16–19] and testing of new NMR experimental methods also require experimental data from assigned compounds for validation. This work reports a validated set of experimental NMR ^1H and ^{13}C scalar coupling constants and chemical shifts for a selection of representative complex organic structures and an example application of such a dataset in benchmarking the calculation of NMR parameters used for 3D structural determination by density functional theory (DFT).

Experimental ^1H and ^{13}C chemical shift values abound in open and commercial databases as well as the scientific literature, and while the accuracy of reported chemical shifts is prone to experimental variations (*e.g.* referencing, solvent, temperature, pH) and erroneous reporting (typographical or chemical assignment errors being relatively common), the quantity of experimental chemical shifts reported in the literature means sufficient data can usually be sourced for validation studies. On the other hand, experimental ^1H–^1H scalar coupling constants ($^nJ_{HH}$) are more prone to issues, with low precision reporting (precision to the nearest 0.5 Hz is common), misassignment of couplings in complex multiplets or diastereotopic protons, and indeed the multiplicity, individual J values and/or their assignments are often not reported at all. The situation is even worse for ^1H–^{13}C scalar coupling constants ($^nJ_{CH}$) as these values are rarely reported, and when they are it is typically only selected values for one or two protons or carbons in a given compound, and the values are rarely validated for accuracy. The largest published collections of $^nJ_{CH}$

[a]*University of Bristol, School of Chemistry, Cantock's Close, Bristol, BS8 1TS, UK. E-mail: craig.butts@bris.ac.uk*
[b]*JEOL (UK) Ltd, Welwyn Garden City, UK*
[c]*C4X Discovery, Manchester One, 53 Portland Street, Manchester, M1 3LD, UK*

†Electronic supplementary information (ESI) available: Experimental and computed NMR parameters for all compounds, including cartesian coordinates used for computation. See DOI: https://doi.org/10.1039/d5an00240k

that we are aware of, contain 100–300 values[20] focused on structurally related compounds that may require chemical synthesis to reproduce the full set and without validation of the accuracy or assignments.[5,21] At the same time, multiple-bond ($^nJ_{CH}$) couplings are becoming increasingly recognised as valuable for elucidating chemical structure.[22–24] They are often complementary to $^nJ_{HH}$ for determining conformation and stereochemistry but can additionally probe quaternary carbon centres and connect spin-systems separated by non-protonated carbons and heteroatoms, that are inaccessible with $^nJ_{HH}$ alone.

We have recently been interested in the application of $^nJ_{CH}$ values in a series of elucidations of 3D structure.[25,26] However, it was not initially clear to us what methods (either experimental or computational) were the most reliable for this, so we have previously evaluated the accuracy of a variety of experimental methods to measure $^nJ_{CH}$ for two model compounds, strychnine and camphor.[27] It was found that EXSIDE[28] and IPAP-HSQMBC[29,30] pulse sequences were both able to extract $^nJ_{CH}$ with relatively high accuracy (<0.4 Hz average deviations), with the latter being substantially more time-efficient when measuring values for multiple protons in the same study. With these tools in hand, it becomes plausible to start developing robust and validated datasets of NMR parameters which include $^nJ_{CH}$ as part of these.

Herein, we have measured, assigned and validated $^nJ_{CH}$, along with $^nJ_{HH}$, ^{1}H and ^{13}C chemical shifts for fourteen organic molecules (Fig. 1), to establish these values with a known estimate of accuracy.[20,27] Crucially, the assignments (including to diastereotopic nuclei) of these NMR parameters were verified by comparison with DFT-calculated values and were subsequently used to test the accuracy of methods for the conversion of DFT-calculated magnetic shielding tensors (MST) into chemical shifts.[31–33] This assignment and validation process included calculating the 3D structures of the molecules, which are also included in the dataset for completeness.

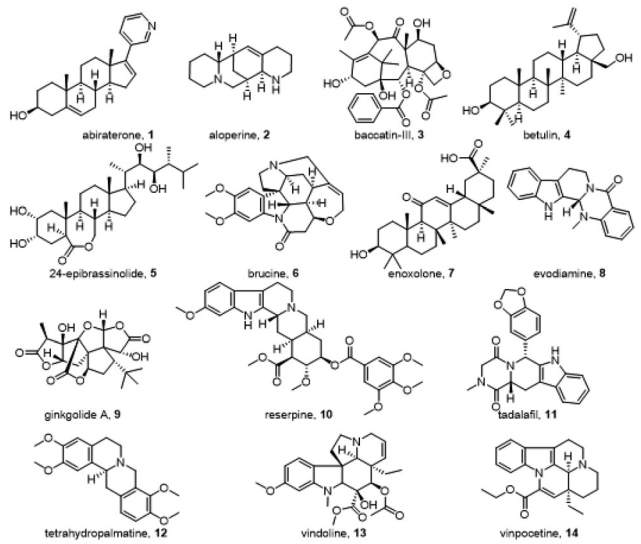

Fig. 1 The set of molecules under study, Cartesian coordinates for the 3D structures are provided in the ESI (Table S16†).

Results and discussion

Fourteen compounds (Fig. 1) were selected as readily accessible and commercially available at time of publication, relatively complex small organic molecules with well-defined 3D structures. The compounds provide a mixture of functionalities, atom hybridisation and a mixture of rigid and flexible substructures. They provide sufficient structural diversity for a reasonable test for new experimental or computational methods to measure/calculate NMR parameters, but without being too extensive or demanding for ready use in validation studies. The make-up of experimental data determined are summarised in Table 1 (full lists of values and assignments are provided in the ESI, Tables S10–S13†).

Experimental ^{1}H and ^{13}C chemical shifts

The complete set of NMR parameters comprises 332 ^{1}H and 336 ^{13}C chemical shifts, derived from multiplet simulations of ^{1}H spectra and direct measurement from ^{13}C{^{1}H} spectra respectively. The ^{1}H chemical shifts range from 0.417 to 11.069 ppm and were measured for 316 ^{1}H attached to carbon, 4 to nitrogen and 12 to oxygen (Fig. 2). The majority of the ^{1}H chemical shifts correspond to ^{1}H attached to sp^3 centres (280 sp^3 in comparison to 52 sp^2). The ^{13}C chemical shifts range from 7.577 to 203.130 ppm measured from 218 sp^3 centres

Table 1 Summary of measurable ^{1}H and ^{13}C chemical shifts (δ) and long-range proton-proton ($^nJ_{HH}$) and proton-carbon scalar couplings ($^nJ_{CH}$). Where (a) is the complete set of data for **1–14** and (b) is the subset of the data (**1**, **3–7**, **9–14**) that is suitable for benchmarking applications, the selection criteria for this subset are discussed in detail in the main text. MCP (multiple coupling pathways) indicates that coupling pathways of different lengths are possible *e.g.* $^3J_{CH}$ and $^4J_{CH}$ in ring systems

	(a) Complete set		(b) Benchmarking subset	
	Total	Breakdown	Total	Breakdown
^{1}H δ	332	280 sp^3, 52 sp^2	172	146 sp^3, 46 sp^2
^{13}C δ	336	218 sp^3, 118 sp^2	237	163 sp^3, 74 sp^2
$^nJ_{HH}$	300	63 $^2J_{HH}$, 200 $^3J_{HH}$, 28 $^4J_{HH}$, 9 $^{5+}J_{HH}$	205	49 $^2J_{HH}$, 134 $^3J_{HH}$, 16 $^4J_{HH}$, 6 $^{5+}J_{HH}$
$^nJ_{CH}$	775	241 $^2J_{CH}$, 481 $^3J_{CH}$, 79 $^4J_{CH}$, 4 $^{5+}J_{CH}$, 30 MCP	570	187 $^2J_{CH}$, 337 $^3J_{CH}$, 70 $^4J_{CH}$, 3 $^{5+}J_{CH}$, 27 MCP

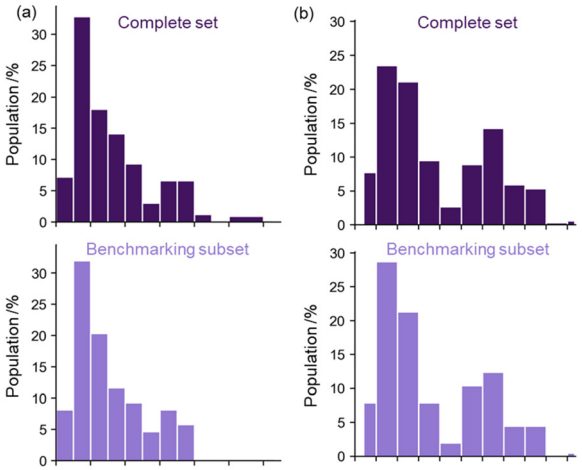

Fig. 2 Distribution of experimentally measured (a) ^{1}H and (b) ^{13}C chemical shifts. Where dark purple indicates the complete set of data for **1–14** and light purple the subset of the data that is suitable for benchmarking applications.

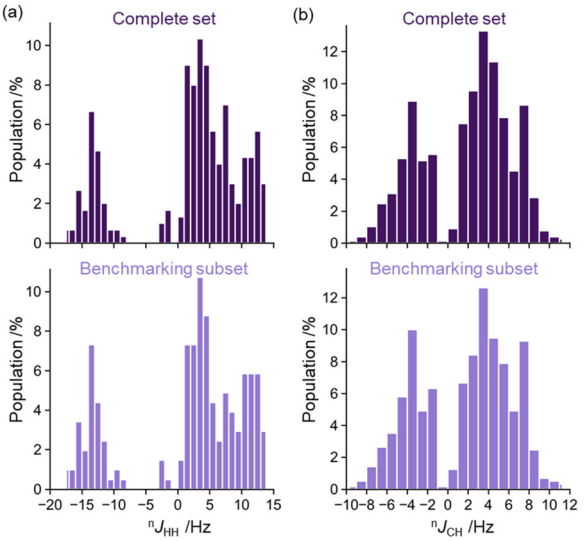

Fig. 3 Distribution of experimentally measured (a) $^{n}J_{HH}$ and (b) $^{n}J_{CH}$ scalar couplings. Where dark purple indicates the complete set of data for **1–14** and light purple the subset of the data that is suitable for benchmarking applications. Only the magnitudes of the couplings were experimentally measured, the signs reported in this figure were calculated by DFT.

and 118 sp^2 centres including aromatic, alkene and carbonyl carbons. Compounds including sp hybridised carbons were not a focus here, given our primary focus on $^{n}J_{CH}$ values and 3D structure determination, which are not especially relevant for these centres.

Experimental ^{1}H–^{1}H scalar coupling constants, $^{n}J_{HH}$

A total of 300 $^{n}J_{HH}$ (Table 1) were measured from multiplet simulation of ^{1}H spectra performed using C4X Assigner,[34] anti-Z-COSY[35,36] or PIP-HSQC[29] as described in the Methods section. This combination of techniques maximised the number of measurable couplings which otherwise would have been lost to overlap or complications from strong coupling. The $^{n}J_{HH}$ range from 0.8 to 17.5 Hz (Fig. 3(a)) with the majority of the $^{n}J_{HH}$ measured between ^{1}H separated by three-bonds (200) but with a substantial number of two-bond (63) and four-bond or more (37) couplings also extracted.

Experimental ^{1}H–^{13}C scalar coupling constants, $^{n}J_{CH}$

It is notable that 775 $^{n}J_{CH}$ values could be measured for compounds **1–14** (Fig. 1) – this is a much higher number than for the corresponding $^{n}J_{HH}$ (300) and highlights our interest in these parameters, as a large quantity of data can be captured if scalar couplings to ^{13}C are included in chemical structure elucidation/verification studies. These were extracted from IPAP-HSQMBC, since this method offers an optimum balance of reliability and accuracy in $^{n}J_{CH}$ measurement with efficiency of spectrometer time for these parameters.[27] The $^{n}J_{CH}$ values ranged from 0.7 to 11.3 Hz (Fig. 3(b)) with the majority of $^{n}J_{CH}$ measured between ^{1}H/^{13}C separated by three-bonds (481) but again with substantial numbers of couplings across two-bonds (241), or four or more bonds (83). Another interesting feature which is not uncommon for ^{1}H–^{13}C scalar couplings is the relative abundance of values (30) for which the two nuclei are connected by more than one bonding pathway of four-bonds or less. For example a ^{1}H and a ^{13}C which are 3 bonds apart in a five-membered ring, are also 4 bonds apart if one traces the bonding in the opposite direction around the ring. While this does not affect the results presented here, it is notable that this property of rings of 5-or-less atoms obviously complicates methods for empirical prediction of ^{1}H–^{13}C couplings where the effect of only a single pathway for the coupling is typically considered.

Validation of experimentally measured NMR parameters

DFT calculations of the NMR ^{1}H and ^{13}C chemical shifts and ^{1}H–^{1}H and ^{1}H–^{13}C scalar coupling constants were also performed on compounds **1–14** in order to confirm assignments of chemical shifts and couplings to each nucleus. To account for the flexibility in each structure, initial molecular mechanics conformational searches were conducted to find the conformers of each compound that might be populated to any significant extent at room temperature. Subsequent DFT geometry optimisation, zero-point energy corrections and NMR parameter calculations were conducted with the mPW1PW91 functional and 6-311(d,p) basis set (full details in the Methods section) for each conformer before Boltzmann population weighting was applied to the computed parameters in order to predict ensemble-averaged values. Where gross deviations between the experiment and calculated values were observed then extraction of values from spectra were re-checked and corrected where appropriate ensuring that the 2D NMR spectra agreed with any changes in assignment.

During the process of DFT-validation of the assignments the risks of relying on human-assigned NMR parameters from the literature were highlighted. We simulated a rough-and-

ready assignment process for the initial assignment of the experimental NMR data for compounds **1–14** by providing the data as training exercises for newly recruited analysts. Validation against the DFT data found that around one tenth of chemical shift assignments and one sixth of values/assignments of coupling constants were erroneous in our initial assignment process. In particular, the δ^{13}C assignment of aromatic rings from HMBC spectra (where correlations for aromatic 2-bond couplings are often not observed, but are observed for 3-bond couplings) and ^{1}H assignment of diastereotopic protons (where the 3D structure must be understood in order to definitely assign the protons) is prone to human error. This highlights the need for properly validated experimental NMR data for use in developing/testing of experimental and computational methodologies.

The final, validated and assigned NMR parameters for the 14 molecules can be found in Tables S10–S13 of the ESI.†

Application to DFT benchmarking

In order to demonstrate one potential application of these data, we use them to benchmark our DFT NMR prediction method.

To achieve this, firstly a subset of the experimental data was needed, which was suitable for benchmarking against calculated values. As experimental data are conformationally averaged, while DFT data are on single geometry structures, this subset should be minimally impacted by conformational dynamics (and thus the need to estimate conformer populations), ambiguity in assignments and chemical exchange. Consequently, a series of criteria were applied when selecting appropriate experimental data from **1–14**:

(1) The assignment of the nucleus and its associated NMR parameters must be unambiguous from the spectroscopic data.

(2) The nucleus must not be part of, or adjacent to, a freely rotating group such as an ethyl or methoxy group. Where such a group was conjugated to an adjacent π-electron system however, the entire conjugated system was included as the conjugated conformer dominates the NMR behaviours.

(3) For each molecule, the MM/QM conformational search performed should not show a significant population of minor conformers in the fused ring portions of the molecule (major conformer >90% population at 298 K based on DFT-predicted free energy). This excluded all values for compounds **2** and **8** where the primary ring conformations were predicted to be populated to <70%.

(4) Scalar couplings and chemical shifts of protons attached to N or O were excluded. The dependence of these experimental values on sample conditions (pH, temperature, concentration, presence of water) is challenging to adequately reproduce with DFT.

The final benchmarking subset (provided in ESI Tables S10–S13† with details for each excluded value) contains 172 ^{1}H and 237 ^{13}C chemical shifts, 205 $^{n}J_{HH}$ and 570 $^{n}J_{CH}$ from compounds **1**, **3–7** and **9–14** (Table 1). Fig. 4 shows the comparison of the experimental ^{1}H/^{13}C chemical shifts and $^{n}J_{HH}$/$^{n}J_{CH}$ coupling constants to their DFT-calculated values. Although DFT calculations capture the sign of scalar coupling constants, the absolute values were compared as the experimental methods used here do not extract the sign.

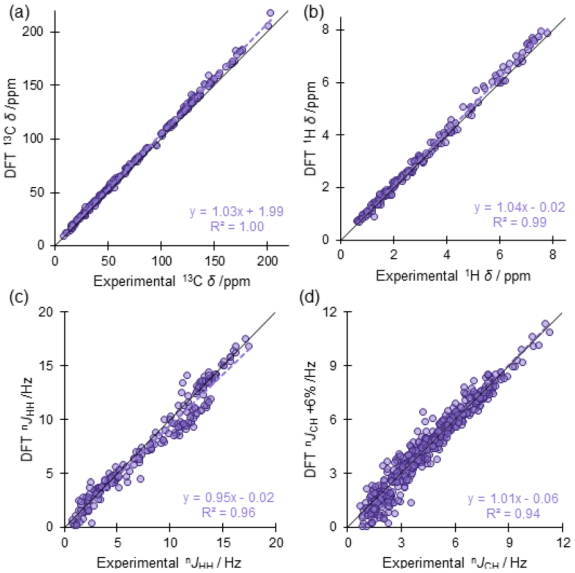

Fig. 4 Comparison of the subset of experimental data suitable for benchmarking with DFT-calculated values, (a) ^{13}C chemical shift (TMS conversion), (b) ^{1}H chemical shift (TMS conversion) (c) $^{n}J_{HH}$ and (d) $^{n}J_{CH}$.

The comparisons of experimental and DFT-calculated (mPW1PW91/6-311 g(d,p)) $^{n}J_{HH}$ and $^{n}J_{CH}$ (Fig. 4(c and d)) show reasonable correlation with no significant outliers. However, the accuracy of the computed $^{n}J_{HH}$ values in particular is relatively low, with a mean absolute deviation (MAD) of 0.75 Hz and standard deviation (SD) of 0.93 Hz for the 205 scalar couplings in the benchmarking subset (Table 2), this is in line with the accuracy reported by Bally and Rablen in 2011[15]

The accuracy of $^{n}J_{CH}$ coupling constants calculated by DFT is better than $^{n}J_{HH}$ with MAD of 0.44 Hz and SD of 0.50 Hz (Table 2) for the raw DFT-calculated values. Our previous work on accurate experimental $^{n}J_{CH}$ measurements, limited to example molecules strychnine and camphor, showed that the mPW1PW91/6-311 g(d,p) level of theory systematically underpredicts $^{n}J_{CH}$ by ~6%.[27] The benchmarking subset here confirmed this observation, as correcting the DFT-calculated values by this same empirical factor improved the MAD to 0.38 Hz while the standard deviation (which is mostly sensitive to dispersion of the errors) remains at ~0.5 Hz. These corrected MAD/SD values are in

Table 2 Summary statistics comparing DFT-calculated scalar couplings to the measured experimental data from the benchmarking subset: MAD (mean absolute deviation) and SD (standard deviation of the errors)

NMR parameter	MAD/Hz	SD/Hz	Total
$^{n}J_{HH}$, no scaling	0.75	0.93	205
$^{n}J_{CH}$, no scaling	0.44	0.50	570
$^{n}J_{CH}$, 6% scaling	0.38	0.52	570

line with the data we reported previously for strychnine and camphor (0.38 Hz MAD and 0.49 Hz SD) in that report.

We also used this benchmarking dataset to test referencing/scaling methods for DFT-based chemical shift predictions. DFT-calculations do not directly provide chemical shifts, but instead compute magnetic shielding tensors (MST). Therefore, for solution-state measurements, the isotropic component of the MST is converted, by some referencing/scaling process, to produce a chemical shift. Several different referencing/scaling methods have been reported for conversion of MST to chemical shifts, the benchmarking subset of data here was used to demonstrate the outcome for four of these methods.

TMS-only referencing of δ. The simplest method used here referenced all the DFT-calculated MST values from the benchmarking subset relative to the ^{1}H and ^{13}C MSTs calculated for tetramethylsilane (TMS) with the same DFT method.[31] Fig. 4(a and b) shows that this provides a reasonable correlation and is the most general method: it is easily applied across different solvents and does not require any experimental data. However, it suffers from the systematic error arising from any miscalculation in the MST for TMS as well as any deviation from 1 : 1 scaling of the computed MST to experimental chemical shifts in solution. The corresponding statistics reported in Table 3 ("TMS-only") for this method confirm the low accuracy, as it shows the highest MAD/SD of the four conversion methods (Table 3: ^{1}H: 0.14/0.16 ppm; ^{13}C: 4.3/2.3 ppm).

Internal scaling of δ. In reports of the DP4 analysis of NMR chemical shifts, Goodman *et al.*[31] use an internal-scaling method whereby the experimental data is used to calculate a line-of-best fit to the TMS-referenced DFT-calculated chemical shifts and the calculated values are subsequently corrected based on this line-of-best fit. In principle, this removes any systematic referencing error based on TMS (as the data is now internally referenced to all the experimental data in the benchmarking dataset) and also any absolute scaling error in the shielding tensor itself. The line-of-best fit corresponds to the slope and intercepts shown in Fig. 4(a and b), application of these to the TMS-only chemical shifts to give the "Internal-scaling" values in Table 3. By definition, this method must result in the best fit of any methods tested for this particular set of compounds, and thus unsurprisingly it shows the lowest MAD/SD for both ^{13}C and ^{1}H (Table 3: ^{1}H: 0.11/0.14 ppm; ^{13}C: 1.2/1.7 ppm). However, this method risks overfitting to the internal dataset and thus is not suitable for experimental datasets consisting of only a few values. It has been primarily applied to discriminate diastereomers using the differences between multiple calculated data sets, such as in Goodman's DP4 approach, where absolute accuracy is not the goal.

External scaling of δ (all hybridisations). Scaling factors for MSTs can also be generated from an independent experimental study on a suite of sensibly diverse chemical structures, (referred to as "external-scaling" in Table 3) as described by Tantillo *et al.*[32] These should be robust to a wider range of chemical space and should be used when there are too few datapoints for reliable internal-scaling. However, these external scaling factors must then be calculated for the entire suite of diverse experimental molecules, using the same computational method that is used for the compounds of interest in any given study. In this report the DFT calculations (using the method above: mPW1PW91/6-311 g(d,p) with implicit solvent model (IEFPCM) for DMSO or chloroform) were therefore performed for an independent DFT dataset of 40 ^{1}H and 45 ^{13}C chemical shifts from 23 molecules previously reported by Pierens for this purpose[33] and derived from experimental data reported by Gottlieb *et al.* and Fulmer *et al.* which contain chemical shifts measured in a range of solvents including $CDCl_3$ and DMSO-d6.[37,38] The application of the resulting external-scaling factors achieved a significant improvement in accuracy relative to the use of TMS-only scaling (Table 3: ^{1}H: 0.11/0.14 ppm; ^{13}C: 1.5/1.8 ppm) and only slightly lower than that achieved with the overfitted internal scaling method.

External scaling of δ (separated hybridisations). A fourth approach can be considered, based on the recommendation of Tantillo *et al.* to separate the treatment of sp^2/sp^3 ^{13}C chemical shifts for the generation of scaling factors. However, the relatively narrow range of chemical shifts for sp^3 (~70 ppm) and sp^2 carbons (~100 ppm) in the Pierens dataset makes the slopes of these plots less reliable (effectively an underfitting to the experimental dataset). This is seen in the slight reduction in accuracy for this ("external-scaling (^{13}C sp^2/sp^3 separated)") methods in Table 3 (^{13}C: 1.5/2.0 ppm).

One can conclude from these four tests, that the external scaling approach is relatively robust, but where sufficient experimental data is available in order to avoid overfitting, then the internal scaling approach will offer slight improvements in accuracy in some cases.

Table 3 Summary statistics comparing DFT-calculated chemical shifts to the measured experimental data from the benchmarking subset. Where, MAD (mean absolute deviation) and SD (standard deviation of the errors)

Method	^{1}H δ: 172 values MAD ± SD/ppm	^{13}C δ: 237 values MAD ± SD/ppm
TMS-only	0.14 ± 0.16	4.3 ± 2.3
Internal-scaling	0.11 ± 0.14	1.2 ± 1.7
External-scaling	0.11 ± 0.14	1.5 ± 1.8
External-scaling (^{13}C sp^2/sp^3 separated)		1.5 ± 2.0

Conclusions

A dataset of ^{1}H (332) and ^{13}C (336) NMR chemical shifts and $^{n}J_{HH}$ (300) and $^{n}J_{CH}$ (775) scalar coupling constants for fourteen relatively complex organic molecules have been measured experimentally and assigned, with any assignment ambiguities noted. The 3D structures and rigidity of each molecule were established by MM and DFT calculations, and rigid portions of the molecules were identified to establish a benchmarking subset of these NMR parameters that are suitable for comparison of computed and experimental values. This benchmarking

dataset were demonstrated in the validation and benchmarking of the mPW1PW91/6-311 g(d,p) DFT functional and basis set combination. This provides a clear description of the accuracy (with respect to experiment) of the DFT-calculated coupling constants taken directly from the calculation, and allows a comparison of scaling methods for DFT-calculated magnetic shielding tensors to produce isotropic chemical shifts.

Data availability

The experimental and computed data supporting this article have been included as part of the ESI.† Raw NMR data files can be found here: **https://doi.org/10.5523/bris.1zczvf3ztyniy2phuwlfl8vb8l**.

Conflicts of interest

There are no conflicts to declare.

Acknowledgements

We thank of the Advanced Computing Research Centre, University of Bristol (**https://www.bris.ac.uk/acrc/**) for access to high performance computing resources.

References

1 Spectral Database of Organic Compounds: **https://sdbs.db.aist.go.jp/** Update 2018.06.14.
2 C. Steinbeck, S. Krause and S. Kuhn, *J. Chem. Inf. Comput. Sci.*, 2003, **43**, 1733–1739.
3 J. W. Emsley and L. Phillips, *Prog. Nucl. Magn. Reson. Spectrosc.*, 1971, **7**, 1–520.
4 J. W. Emsley, L. Phillips and V. Wray, *Prog. Nucl. Magn. Reson. Spectrosc.*, 1976, **10**, 83–752.
5 P. E. Hansen, *Prog. Nucl. Magn. Reson. Spectrosc.*, 1981, **14**, 175–295.
6 (*a*) M. Karplus, *J. Am. Chem. Soc.*, 1963, **85**, 2870–2871; (*b*) C. Altona, eMagRes, 2007, DOI: **10.1002/9780470034590.emrstm0587**; (*c*) A. Navarro-Vázquez, R. Santamaría-Fernández and F. J. Sardina, *Mag. Reson. Chem.*, 2018, **56**, 505–512.
7 **https://nmrpredict.orc.univie.ac.at**.
8 **https://www.acdlabs.com/products/adh/nmr/nmr_pred/**.
9 K. A. Blinov, Y. D. Smurnyy, T. S. Churanova, M. E. Elyashberg and A. J. Williams, *Chemom. Intell. Lab. Syst.*, 2009, **97**, 91–97.
10 C. Venkata, M. J. Forster, P. W. A. Howe and C. Steinbeck, *PLoS One*, 2014, **9**, e111576.
11 (*a*) W. Gerrard, L. A. Bratholm, M. J. Packer, A. J. Mulholland, D. R. Glowacki and C. P. Butts, *Chem. Sci.*, 2020, **11**, 508; (*b*) Y. Guan, S. V. Shree Sowndarya, L. C. Gallegos, P. C. St. John and R. S. Paton, *Chem. Sci.*, 2021, **12**, 12012.
12 E. Benassi, *J. Comput. Chem.*, 2017, **38**, 87–92.
13 D. Flaig, M. Maurer, M. Hanni, K. Braunger, L. Kick, M. Thubauville and C. Ochsenfeld, *J. Chem. Theory Comput.*, 2014, **10**, 572–578.
14 R. Suardíaz, C. Pérez, R. Crespo-Otero, J. M. García de la Vega and J. S. Fabián, *J. Chem. Theory Comput.*, 2008, **4**, 448–456.
15 T. Bally and P. R. Rablen, *J. Org. Chem.*, 2011, **76**, 4818–4830.
16 A. Howarth, K. Ermanis and J. M. Goodman, *Chem. Sci.*, 2020, **11**, 4351.
17 Z. Huang, M. S. Chen, C. P. Woroch, T. E. Markland and M. W. Kanan, *Chem. Sci.*, 2021, **12**, 15329–15338.
18 E. Troche-Pesqueira, C. Anklin, R. R. Gil and A. Navarro-Vázquez, *Angew. Chem., Int. Ed.*, 2017, **56**, 3660–3664.
19 A. Navarro-Vázquez, R. R. Gil and K. J. Blinov, *Nat. Prod.*, 2018, **81**, 203–210.
20 G. K. Pierens, T. K. Venkatachalam and D. C. Reutens, *Mag. Reson. Chem.*, 2016, **54**, 941–946.
21 A. G. Kutateladze and O. A. Mukhina, *J. Org. Chem.*, 2015, **80**, 10838–10848.
22 A. V. Buevich and M. E. Elyashberg, *Anal. Sci.*, 2020, **58**, 594–606.
23 A. V. Buevich, J. Saurí, T. Parella, N. De Tommasi, G. Bifulco, R. T. Williamson and G. E. Martin, *Chem. Commun.*, 2019, **55**, 5781.
24 J. Saurí, S. T. S. Chan, A. V. Buevich, K. R. Gustafson, R. T. Williamson and G. E. Martin, *Planta Med.*, 2015, **81**, PQ32.
25 J. Wu, P. Lorenzo, S. Zhong, M. Ali, C. P. Butts, E. L. Myers and V. K. Aggarwal, *Nature*, 2017, **547**, 436–440.
26 M. Burns, S. Essafi, J. R. Bame, S. P. Bull, M. P. Webster, S. Balieu, J. W. Dale, C. P. Butts, J. N. Harvey and V. K. Aggarwal, *Nature*, 2014, **513**, 183–188.
27 C. L. Dickson, C. D. Blundell, C. P. Butts, A. Felton, A. Jeffreys and Z. Takacs, *Analyst*, 2017, **142**, 621–633.
28 V. V. Krishnamurthy, *J. Magn. Reson., Ser. A*, 1996, **121**, 33–41.
29 L. Castañar, J. Saurí, R. T. Williamson, A. Virgili and T. Parella, *Angew. Chem., Int. Ed.*, 2014, **53**, 8379–8382.
30 G. D. Poggetto, J. V. Soares and C. F. Tormena, *Anal. Chem.*, 2020, **92**, 14047–14053.
31 S. G. Smith and J. M. Goodman, *J. Am. Chem. Soc.*, 2010, **132**, 12946–12959.
32 M. W. Lodewyk, M. R. Siebert and D. J. Tantillo, *Chem. Rev.*, 2011, **112**, 1839–1862.
33 G. K. Pierens, *J. Comput. Chem.*, 2014, **35**, 1388–1394.
34 Unpublished, proprietary in-house software.
35 H. Oschkinat, A. Pastore, P. Pfändler and G. Bodenhausen, *J. Magn. Reson.*, 1986, **69**, 559–566.
36 A. J. Pell, R. A. E. Edden and J. Keeler, *Mag. Reson. Chem.*, 2007, **45**, 296–316.
37 H. E. Gottlieb, V. Kotlyar and A. Nudelman, *J. Org. Chem.*, 1997, **62**, 7512–7515.
38 G. R. Fulmer, A. J. M. Miller, N. H. Sherden, H. E. Gottlieb, A. Nudelman, B. M. Stoltz, J. E. Bercaw and K. I. Goldberg, *Organometallics*, 2010, **29**, 2176–2179.

